International Journal of Academic Research and Reflection Vol. 3, No. 5, 2015
ISSN 2309-0405

THE EFFECT OF REVOLUTION PER MINUTE (RPM) ON IRON OXIDE NANOPARTICLES (Fe_3O_4NPS) SYNTHESIS THROUGH DIRECT OXIDATIVE ALKALINE HYDROLYSIS

Orlando Ketebu
Niger Delta University
NIGERIA

Rhoda Gumus
Niger Delta University
NIGERIA

Oyinkepreye Orodu
Covenant University
NIGERIA

ABSTRACT

Iron oxide nanoparticles are useful particles in many fields such as medical, biomedical and environmental applications. The nature, sizes, purity and composition of these nanoparticles plays important role in their applications especially in biomedical application. This allows for the efficient use of the unique properties of iron oxide nanoparticles for analysis. This paper reports the effect of revolution per minute on the synthesis of iron oxide nanoparticles through oxidative alkaline hydrolysis of iron salt (iron II sulphate). X-ray diffraction (XRD), X-ray photoelectron spectroscopy (XPS) and transmission electron microscopy (TEM) were used in the analysis of the nanoparticles. The result shows that increase revolution per minute decreases the iron oxide nanoparticles sizes (Fe_3O_4 Nps) with the smallest particle size of 50 nm at 1500 rpm and biggest size of 74 nm for the control sample (without rpm). The nanoparticles from TEM analysis have cubic structure at constant salt concentration of 0.035M. And no significant change in the composition of the nanoparticles synthesized at 200 rpm and the control was observed aside change in their particle size. Nanoparticles synthesized at high revolution per minute of 500 and 1500 rpm showed traces of hematite (α-Fe_2O_3) and iron oxy hydroxide (γ-FeOOH) as impurities mixed with iron oxide nanoparticles.

Keywords: Iron oxide nanoparticles; X-ray diffraction, X-ray photoelectron spectroscopy, Revolution per minute, Transmission electron microscopy.

INTRODUCTION

Iron oxide nanoparticles magnetite (Fe_3O_4) or maghemite (γ-Fe_2O_3) plays important role in medical and biomedical applications such as hyperthermia therapy, drug delivery and magnetic resonance imaging.(Gupta and Gupta, 2005; Gupta *et al.*, 2007; Jain *et al.*, 2008) . There use depends on their sizes, nature, stability and purity which are influenced by their mode of synthesis. This in turn affects their magnetic properties, potency and sensitivity in their applications. Iron oxide nanoparticles can be synthesized through different synthetic route such as sonochemical reactions (Abu Mukh-Qasem and Gedanken, 2005; Zhang *et al.*, 2010; Dai *et al.*, 2013; Zhu *et al.*, 2013)., hydrothermal reactions and thermal deposition (Ge *et al.*, 2009; Li *et al.*, 2011; Liu *et al.*, 2011; Junejo *et al.*, 2013; Panchal *et al.*, 2013), co-precipitation (Lyon *et al.*, 2004; Qu *et al.*, 2010; Behera, 2011; Salehizadeh *et al.*, 2012; Wang *et al.*, 2013), microemulsions (Xu *et al.*, 2010; Ji *et al.*, 2011; Mert *et al.*, 2013) , flow injection and electro spray method.(Laurent *et al.*, 2008). Magnetite nanoparticles (Fe_3O_4) in this paper were synthesis through direct oxidative alkaline hydrolysis of iron II sulphate salt. The process simple involves reacting iron II salt with a strong base (e.g. sodium hydroxide) in the presence of a mild reducing agent (potassium hydroxide) to form iron (II) hydroxide. The iron (II) hydroxide formed is heated and undergoes anaerobic oxidation by the protons of water to form magnetite and molecular hydrogen (Schikorr reaction). The chemical reaction for the synthesis of magnetite and Schikorr reaction are shown in equation1 and 2.

$$6NaOH + 3FeSO_4 \longrightarrow 3Fe(OH)_2 + 3Na_2SO_4 \quad (1)$$

$$3Fe(OH)_2 \longrightarrow Fe_3O_4 + H_2 + 2H_2O \quad (2)$$

Magnetite (Fe_3O_4) is known to be an unstable iron oxide and easily undergoes oxidation in the presence of oxygen to form maghemite (γ-Fe_2O_3) as shown in equation 3.(Rebodos and Vikesland, 2010). The process of oxidation involves the iron II cation Fe^{2+} in the octahedral site of magnetite being oxidized to iron III cation (Fe^{3+}) creating cationic vacancies which helps to maintain the charge balance in maghemite.

$$3Fe_3O_4 + \frac{1}{2}O_2 + 2H^{2+} \longrightarrow 4\gamma\text{-}Fe_2O_3 + Fe^{2+} + H_2O \qquad 3$$

Most often stabilizers are used during magnetite nanoparticles synthesis to improve the mono-dispersity and stability of the particles.

Within the past decade and recently, authors have published works on the synthesis of iron oxide nanoparticles (Fe_3O_4) through oxidative alkaline hydrolysis of iron II sulphate salt. Most attention has been focussed on the synthesis of desired Fe_3O_4 nanoparticles sizes, stabilization and application of the nanoparticles in various fields (Goon *et al.*, 2010) (Mürbe *et al.*, 2008) (Mürbe *et al.*, 2008) (Ma *et al.*, 2013) (Vergés *et al.*, 2008) (Zhou *et al.*, 2010) (Sugimoto and Matijević, 1980). But no work has looked at the synthesis of iron oxide nanoparticles through oxidative alkaline hydrolysis of iron II sulphate salt under the influence of revolution per minute.

The aims of this work is to synthesis magnetite (Fe_3O_4) nanoparticles through oxidative alkaline hydrolysis of iron II sulphate salt and explore the effect of revolution per minute during synthesis on the nature and composition of iron oxide nanoparticles (Fe_3O_4) Nanoparticles. Polyethyleneimine (PEI) a polycation was used as a stabilizing agent and X-ray diffraction and X-ray photoelectron spectroscopy were used in characterizing the nanoparticles.

METHODOLOGY

Materials and chemicals

Polyethyleneimine (branched 25000mw), iron II sulphate heptahydrate >99% ($FeSO_4.7H_2O$) were purchased from Sigma Aldrich (Dorset UK), sodium hydroxide 97% (NaOH), and potassium nitrate 99% (KNO_3) were from Alfa Aesar (Lancashire UK). All chemicals were used as received without further purification. Solutions prepared using Millipore deionised water.

Synthesis of iron oxide core/polyethyleneimine nanoparticles (Fe_3O_4-PEI NPs)

Iron oxide nanoparticles (Fe_3O_4 Np) were synthesized following a method by Goon and co-workers with some modification (Goon *et al.*, 2009). Fixed iron (II) sulphate heptahydrate concentration (0.035M) were added into 80ml of deionized water containing PEI ($500mgl^{-1}$) in a 250ml round bottom flask then sparged for 20 minutes. The mixture was agitated at 200, 500 and 1500 revolution per minute respectively with a mixer. Potassium nitrate (10ml, 2M) was added followed by the addition of sodium hydroxide (10ml, 1M). This result in the formation of iron (II) hydroxide which was heated for 2 hours at 90^0C while constantly mixing at the different revolution per minute and sparging with nitrogen. A black precipitate of iron oxide nanoparticles was formed and washed several times with deionised water. The nanoparticles were finally suspended in 80ml of deionised water at pH 70. The process was repeated without mixing under the influence of rpm and was taken as control.

Characterization of the iron oxide/PEI nanoparticles

X-ray diffraction (XRD) pattern of nanoparticles were obtained using PANalytical X'pert Pro MPD, powered by Philips PW 3040/60 X-ray generator fitted with X'celerator and using Cu Kα radiation with wavelength of 1.54180Å to determine the crystalline structure of the nanoparticles. The nature and core electrons of the Fe_3O_4 nanoparticles were obtained by X-ray photoelectron spectroscopy (XPS) with Thermo Scientific K-α monochromated small spot X-ray Photoelectron Spectrometer system. Transmission electron microscopy analysis (TEM) was carried out with Philips CM200 FEGTEM field emission gun TEM/STEM with supertwin objective lens.

RESULTS

Table 1 Fe_3O_4 nanoparticles synthesized for control and varying revolution per minute

$FeSO_4.7H_2O$ (M)	KNO_3 (M)	NaOH (M)	Temp. (^{0}C)	RPM	Average particle size (nm) XRD
0.035	2.0	1.0	90	-	74
0.035	2.0	1.0	90	200	70
0.035	2.0	1.0	90	500	65
0.035	2.0	1.0	90	1500	50

Figure 1 Fe_3O_4 nanoparticles synthesized with PEI showing paramagnetic properties before and after magnetic separation (a) and (b) control, (c) at 1500 rpm and (d) TEM image of control

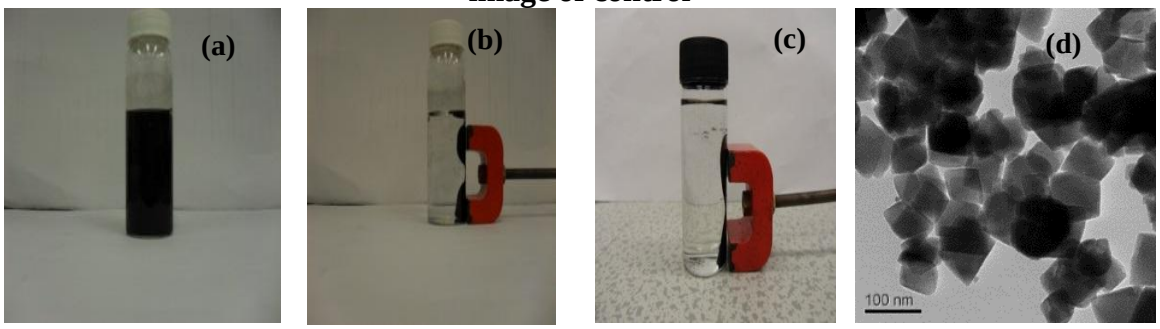

Figure 2 Fe_3O_4 nanoparticles XPS analysis showing (a) 2p core electrons (b) 1s core electrons of O_2

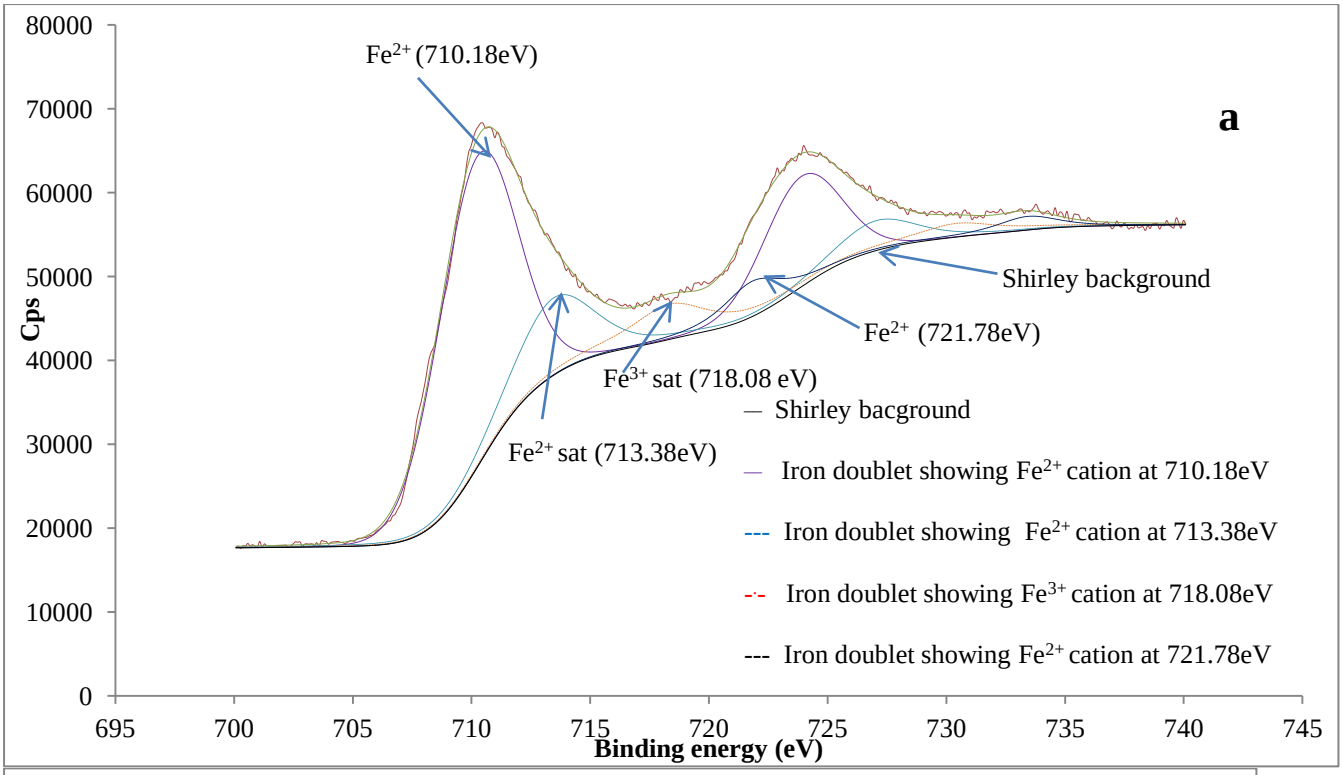

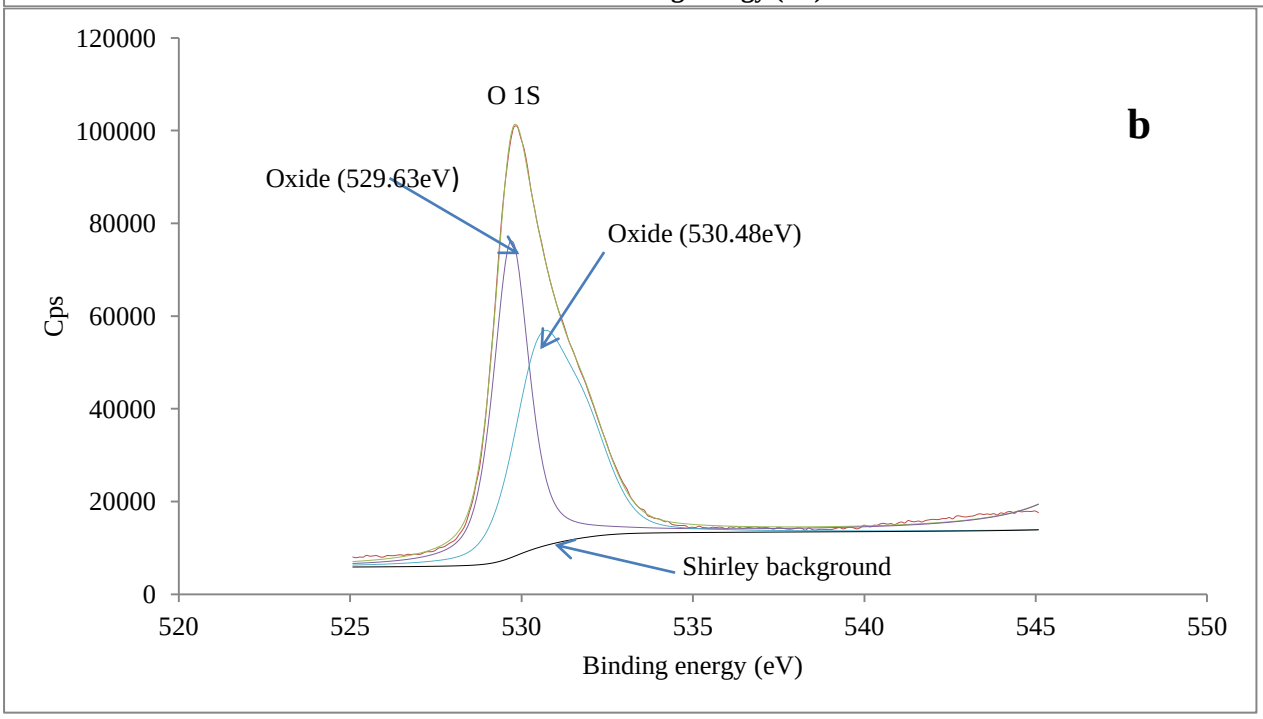

Figure 3 XRD analysis of Fe_3O_4 synthesis at (a) control (b) 200 rpm, (c) 500 rpm and (d) 1500 rpm

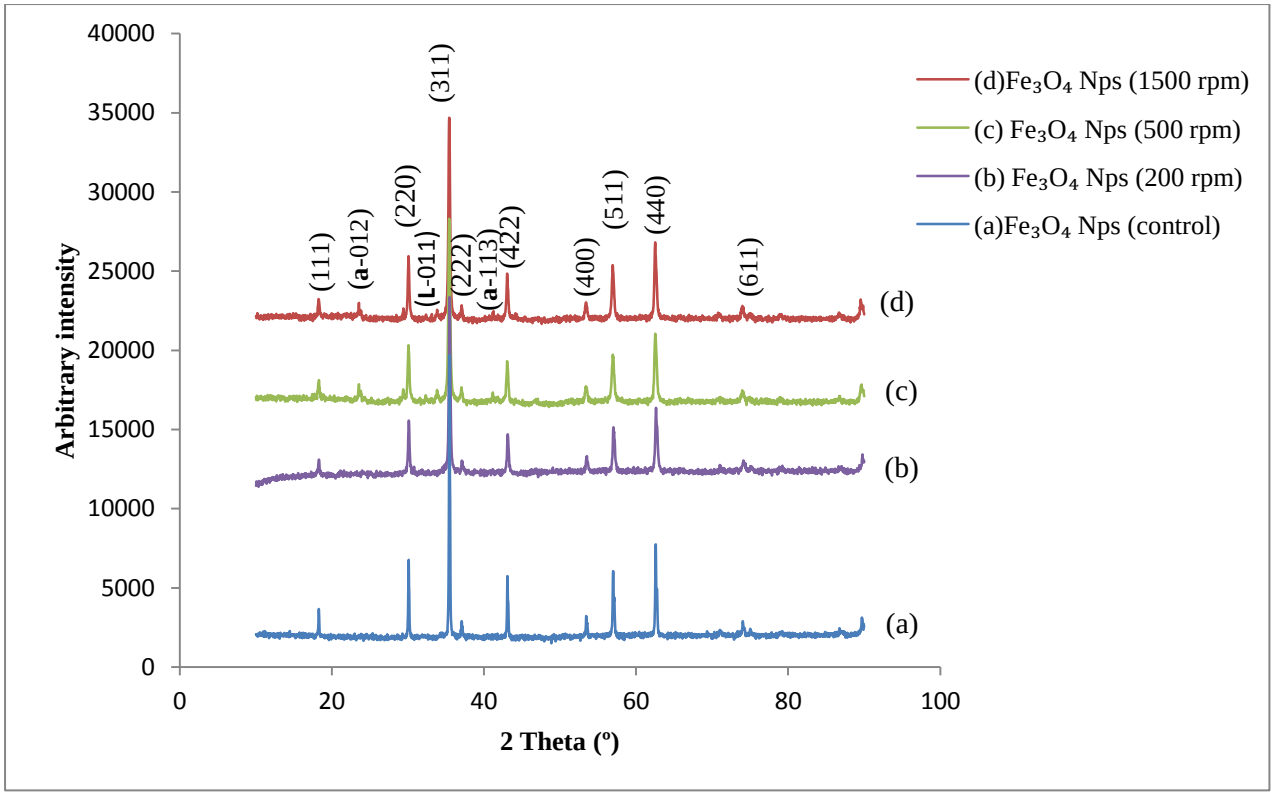

Figure 4 XPS analysis Fe_3O_4 synthesis at (a) control, (b) 200 rpm, (c) 500 rpm, (d) 1500 rpm

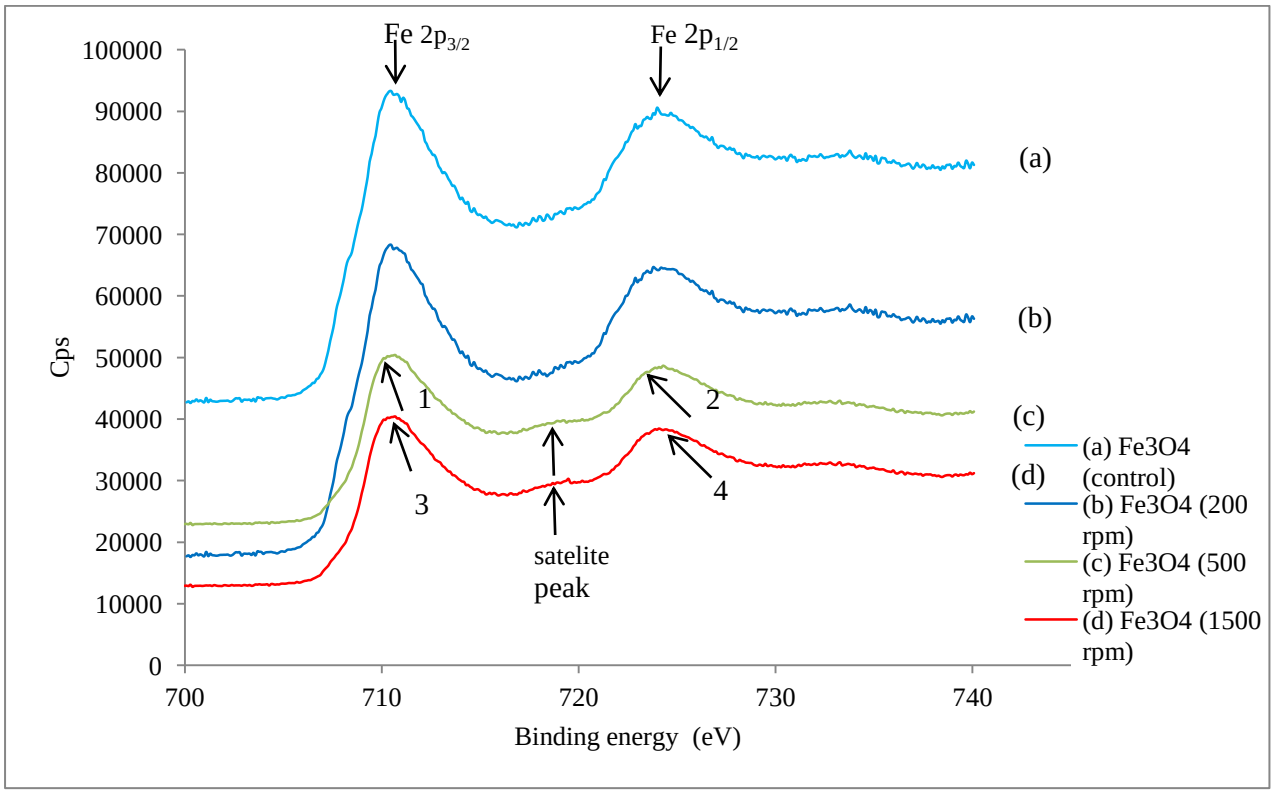

DISCUSSION

Properties of nanoparticles synthesized by varying revolution per minute

Figure1 (a) and (b) shows the paramagnetic behaviour of the iron oxide nanoparticles synthesized without mixing under the influence of revolution per minute (control) in the presence and absence of external magnet. Figure 1 (c) shows the paramagnetic behaviour of the iron oxide nanoparticles synthesized at 1500 rpm. This same behaviour was observed for the nanoparticles synthesized at 200 and 500 revolutions per minute. No difference was observed in the colour of the nanoparticles, although the larger particles were attracted faster to a magnetic field. The paramagnetism is as a result of the 4 unpaired electrons from the 3d orbitals of the iron oxide nanoparticles which align parallel to the magnetic field. Figure 1 (d) shows the TEM image for the control nanoparticles synthesized at 0.035M $FeSO_4$, which indicates that the nanoparticles formed using this iron salt concentration (0.035M $FeSO_4$) are cubic in nature. Figure 2a shows the XPS analysis for the magnetite nanoparticles (control) synthesized at concentration 0.035M $FeSO_4$ in the absence of revolution per minute. The XPS analysis allows for the determination of the elemental composition, chemical state, core electrons and corresponding binding energy of the nanoparticle.

Figure 2a shows the characteristic doublet for iron base compounds indicating the presence of 2p core electrons (Fe $2p_{3/2}$ and $2p_{1/2}$) at the high and low binding energies. The arrows shows the presence of iron II cation (Fe^{2+}) at binding energies of 710.18eV, 713.38eV and 721.78eV and iron III cation (Fe^{3+}) at 718.08eV confirming the formation of magnetite (Fe_3O_4) nanoparticles. Figure 2b also shows that the 1s core electron of oxygen in Fe_3O_4 nanoparticles results only from oxides in the nanoparticles at lower binding peak of 529.58eV and 530.48eV. These same features and 2p core electrons (Fe $2p_{3/2}$ and $2p_{1/2}$) were observed for iron oxide nanoparticles synthesized at 200, 500 and 1500 rpm as shown in Figure 4. Increasing the revolution per minute showed that the nanoparticles crystallite sizes decreased with increase in revolution per minute as shown in table1, with the lowest nanoparticles size of 50 nm obtained at 1500 rpm. The nanoparticles sizes where calculated from the diffraction peaks at (311), (440) and (220) using the Scherrer's formula in equation 4. The size of the crystallite is related with the broadening of peak in the diffraction patterns and can be determined by using the shape factor in the Scherrer equation.

$$\tau = \frac{K\lambda}{\beta cos\theta} \qquad 4$$

Where K is the shape factor, λ is the x-ray wavelength, β is the line broadening at half the maximum intensity in radians, θ is the Bragg's angle and τ is the mean size of the crystalline in ordered domains.

Figure 4 shows the XRD spectrum for Fe_3O_4 control (a) and at 200 (b), 500 (c) and 1500 (d) revolution per minutes. The spectrum shows diffraction peaks of iron oxide (Fe_3O_4) nanoparticles synthesized at constant iron salt concentrations of 0.035 M, and the diffraction peaks (111), (220), (311), (222), (400), (422), (511), (440) and (611) can be indexed to the face-centered cubic structure of magnetite (Fe_3O_4) according to joint committee of powder diffraction standards (JCPDS) number 00-019-0629. The XRD spectrum for 500 and 1500 rpm contains some diffraction peaks that shows the presence of small amount of α-Fe_2O_3 (hematite) and iron oxy hydroxide (γ-FeOOH) also known as Lepidocrocite as impurities present in the Fe_3O_4 nanoparticles. The presence of Lepidocrocite at diffraction peak 011 denoted by **L**-011 might be due to the oxidation of iron II hydroxide ($Fe(OH)_2$) during synthesis enhanced by the mixer spinning at high revolution per minute leading to mixed

ferric and ferrous ions in solution and the formation of magnetite. Lepidocrocite is known to be paramagnetic at room temperature and antiferromagnetic at its Neel temperature of 77K with slightly smaller band gap than goethite at 2.2eV (Hall *et al.*, 1995). The formation of small amount of α-Fe_2O_3 (hematite) at the lower angle might be as a result of larger multiplet splitting of the high spin state $2p_{3/2}$ core electrons during synthesis of Fe_3O_4 nanoparticles caused by higher revolution per minute. Increasing the revolution per minute beyond 1500 to 2000 results in the adhesion and drying of the nanoparticles on the walls of the beaker during synthesis. These made synthesis beyond 1500 rpm impossible to control and leads to loss of the nanoparticles during synthesis.

Figure 4 shows the comparative XPS analysis of the nanoparticles synthesized at higher revolution per minute compared to control. It corroborates the result from the XRD analysis in Figure 3 that the α-Fe_2O_3 (hematite) formed is as a result of multiplet splitting of the high spin core electrons causing the broadening of the Fe2p peaks of magnetite in the 500 and 1500 rpm as indicated by arrows 1, 2 and 3, 4 respectively compared to the control sample and at 200 rpm. The Multiplet splitting of high spin state core electrons is known to be a characteristics step for α-Fe_2O_3 formation.(Mills and Sullivan, 1983; Nasibulin *et al.*, 2009). It is a phenomenon associated with photoelectron peaks caused by an unpaired valence electrons present giving rise to exchange interactions which affect differently the remaining spin-up or spin-down core electrons. In the case of the high spin states the phenomenon is heightened, thus for high spin states of Fe^{II} (iron (II) ion) and Fe^{III} (iron III) a broadening of the Fe2p peaks due to unresolved multiplet splitting is observed.

Also satellite peak were observed at 500 and 1500 rpm synthesis confirming the presence of an oxidized sample in the iron oxide nanoparticles formed.

CONCLUSION

This work shows that iron oxide nanoparticles were successfully synthesized through oxidative alkaline hydrolysis of ferrous ion and that synthesis under the influence of revolution per minute affect the nature and composition of the nanoparticles at high rpm. The result showed that the nanoparticles sizes increases with decreasing revolution per minute and no significant change was observe in the composition for the control and synthesis at 200 rpm. But trace amount of α-Fe_2O_3 and lepidocrocite (γ-FeOOH) were observed as impurities.at 500 and 1500 rpm.

ACKNOWLEDGEMENT

The authors thanks the Petroleum Technology Development Fund (PTDF) for funding this research work

REFERENCES

Abu Mukh-Qasem, R. and Gedanken, A. (2005) . Sonochemical synthesis of stable hydrosol of Fe3O4 nanoparticles, *Journal of Colloid and Interface Science*, 284(2), pp. 489-494.

Behera, S.K. (2011). Facile synthesis and electrochemical properties of Fe3O 4 nanoparticles for Li ion battery anode, *Journal of Power Sources*, 196(20), pp. 8669-8674.

Dai, J. etal. (2013). Facile synthesis of pectin coated Fe3O4 nanospheres by the sonochemical method, *Journal of Magnetism and Magnetic Materials*, 331, pp. 62-66.

Ge, S. etal. (2009) Facile hydrothermal synthesis of iron oxide nanoparticles with tunable magnetic properties, *Journal of Physical Chemistry C*, 113(31), pp. 13593-13599.
Goon, I.Y. etal. (2009) Fabrication and dispersion of gold-shell-protected magnetite nanoparticles: Systematic control using polyethyleneimine, *Chemistry of Materials*, 21(4), pp. 673-681.
Goon, I.Y. etal. (2010) Controlled fabrication of polyethylenimine-functionalized magnetic nanoparticles for the sequestration and quantification of free Cu2+, *Langmuir*, 26(14), pp. 12247-12252.
Gupta, A.K. and Gupta, M. (2005) Synthesis and surface engineering of iron oxide nanoparticles for biomedical applications, *Biomaterials*, 26(18), pp. 3995-4021.
Gupta, A.K. etal. (2007) Recent advances on surface engineering of magnetic iron oxide nanoparticles and their biomedical applications, *Nanomedicine*, 2(1), pp. 23-39.
Hall, P.G., Clarke, N.S. and Maynard, S.C.P. (1995) Inelastic neutron scattering (TFXA) study of hydrogen modes in α-FeOOH (goethite) and γ-FeOOH (lepidocrocite), *Journal of Physical Chemistry*, 99(15), pp. 5666-5673.
Jain, T.K. etal. (2008) Magnetic nanoparticles with dual functional properties: Drug delivery and magnetic resonance imaging, *Biomaterials*, 29(29), pp. 4012-4021.
Ji, Y. etal. (2011) Preparation and characterization of biocompatible magnetic fluids. Chengdu, pp. 384-387.
Junejo, Y., Baykal, A. and Sözeri, H. (2013) Simple hydrothermal synthesis of Fe3O4-PEG nanocomposite, *Central European Journal of Chemistry*, 11(9), pp. 1527-1532.
Laurent, S. etal, (2008) Magnetic iron oxide nanoparticles: Synthesis, stabilization, vectorization, physicochemical characterizations and biological applications, *Chemical Reviews*, 108(6), pp. 2064-2110.
Li, X.M. etal. (2011) Magnetic Fe3O4 nanoparticles: Synthesis and application in water treatment, *Nanoscience and Nanotechnology - Asia*, 1(1), pp. 14-24.
Liu, H.L. etal. (2011) Non-aqueous synthesis of water-dispersible Fe3O 4-Ca3(PO4)2 core-shell nanoparticles, *Nanotechnology*, 22(5).
Lyon, J.L. etal. (2004) Synthesis of Fe oxide Core/Au shell nanoparticles by iterative hydroxylamine seeding, *Nano Letters*, 4(4), pp. 719-723
Ma, M. etal. (2013) Facile synthesis of ultrathin magnetic iron oxide nanoplates by Schikorr reaction, *Nanoscale Research Letters*, 8(1), pp. 1-7.
Mert, E.H. etal. (2013) Synthesis and characterization of magnetic polyHIPEs with humic acid surface modified magnetic iron oxide nanoparticles, *Reactive and Functional Polymers*, 73(1), pp. 175-181.
Mills, P. and Sullivan, J.L. (1983) A study of the core level electrons in iron and its three oxides by means of X-ray photoelectron spectroscopy, *Journal of Physics D: Applied Physics*, 16(5), pp. 723-732.
Mürbe, J., Rechtenbach, A. and Töpfer, J. (2008) Synthesis and physical characterization of magnetite nanoparticles for biomedical applications, *Materials Chemistry and Physics*, 110(2-3), pp. 426-433.
Nasibulin, A. etal. (2009) Simple and rapid synthesis of α- nanowires under ambient conditions, *Nano Research*, 2(5), pp. 373-379.
Panchal, V. etal. (2013) Controlling magnetic properties of iron oxide nanoparticles using post-synthesis thermal treatment, *Applied Physics A: Materials Science and Processing*, pp. 1-8.
Qu, J., Liu, G., Wang, Y. and Hong, R. (2010) Preparation of Fe3O4-chitosan nanoparticles used for hyperthermia, *Advanced Powder Technology*, 21(4), pp. 461-467.
Rebodos, R.L. and Vikesland, P.J. (2010) Effects of oxidation on the magnetization of nanoparticulate magnetite, *Langmuir*, 26(22), pp. 16745-16753.

Salehizadeh, H. etal. (2012) Synthesis and characterization of core-shell Fe 3O 4-gold-chitosan nanostructure, *Journal of Nanobiotechnology*, 10.

Sugimoto, T. and Matijević, E. (1980) Formation of uniform spherical magnetite particles by crystallization from ferrous hydroxide gels, *Journal of Colloid and Interface Science*, 74(1), pp. 227-243.

Vergés, M.A. etal. (2008) Uniform and water stable magnetite nanoparticles with diameters around the monodomain-multidomain limit, *Journal of Physics D: Applied Physics*, 41(13).

Wang, Y.H. etal. (2013) A gold electrode modified with hemoglobin and the chitosan@Fe3O4 nanocomposite particles for direct electrochemistry of hydrogen peroxide, *Microchimica Acta*, 180(7-8), pp. 659-667.

Xu, Y. etal. (2010) Preparation and bio-application of monodisperse composite microspheres with high Fe3O4 content, *Acta Polymerica Sinica*, (11), pp. 1340-1345.

Zhang, X. etal. (2010) Sonochemical synthesis and characterization of magnetic separable Fe 3O4/Ag composites and its catalytic properties, *Journal of Alloys and Compounds*, 508(2), pp. 400-405.

Zhou, X. etal. (2010) Fabrication of Cluster/Shell Fe3O4/Au Nanoparticles and Application in Protein Detection via a SERS Method, *Journal of Physical Chemistry C*, 114(46), pp. 19607-19613.

Zhu, S. etal. (2013) Sonochemical fabrication of Fe3O4 nanoparticles on reduced graphene oxide for biosensors, *Ultrasonics Sonochemistry*, 20(3), pp. 872-880.